Proton transfer in the ground and excited electronic states of [2,2′-bipyridyl]-3,3′-diol. A semiempirical study

Vincenzo Barone,[a] Giuseppe Milano,[a] Laura Orlandini[a] and Carlo Adamo[b]
[a] *Dipartimento di Chimica, Università Federico II, via Mezzocannone 4, I-80134 Napoli, Italy*
[b] *Dipartimento di Chimica, Università della Basilicata, via Nazario Sauro 85, I-85100 Potenza, Italy*

Tautomerization of [2,2′-bipyridyl]-3,3′-diol in several electronic states has been studied theoretically by the semiempirical PM3 method. Particular attention has been devoted to the analysis of proton transfer, which can occur through one- or two-step mechanisms. On the grounds of energetic and structural determinations, it is suggested that this latter mechanism is more effective.

The strong Stokes shift observed in fluorescence spectra can be ascribed to the significant skeletal modifications connected to electronic excitation. A good correspondence has been found between structural characteristics and composition of frontier orbitals.

In recent years there has been great interest in Excited State Proton Transfer (ESPT) reactions, due to the advent of refined spectroscopic techniques, such as picosecond measurements or supersonic jets.[1] These processes usually occur in molecules with functional groups linked by a hydrogen bond; the charge redistribution connected to electronic excitation alters the acid–base properties of these groups, leading to proton transfer along the hydrogen bond in a tautomerization process that is normally fast. ESPT processes are operative in a wide class of molecules and are involved in important processes, ranging from UV photochemical reactions in plants to tautomeric interconversion in nucleic acid bases, to mutagenesis.[2–4] Molecules undergoing ESPT have been also proposed as polymer photostabilizers or laser dyes.[5–7]

As a consequence of this general interest, several studies have been devoted to the analysis of ESPT processes in hetero-aromatic compounds, from both experimental and theoretical points of view.[8–21] In particular, a theoretical analysis of ESPT reactions is not yet a routine task, due to the size of the molecular systems under investigation and to the necessity of characterizing excited electronic states. As a consequence, particular attention has been devoted to proton transfer processes in the ground or, in some cases, in the lowest excited electronic states of relatively small model molecules, such as 2-pyridone.[15–21] Few attempts have been made to investigate larger biological systems undergoing ESPT.[12,14]

The situation is even more involved in those molecules where not only one, but two protons can be transferred *via* an ESPT process.[22,23] One of the molecules is [2,2′-bipyridyl]-3,3′-diol [$BP(OH)_2$, see Fig. 1]. Several experimental studies[24–31] have been devoted to clarifying the spectroscopic behaviour of $BP(OH)_2$ and its relationship with the tautomerization. $BP(OH)_2$ shows a strong Stokes red-shifted fluorescence emission (526 nm) following absorption of a UV photon (at 344 nm).[24] The red shift has been explained in terms of a proton transfer process in an excited electronic state,[24,30] leading to a keto–enol tautomerization. Since both absorption and emission spectra are characterized by single bands, whose maxima are nearly constant in different solvents,[26] a concerted proton transfer (PT) mechanism has been suggested, in which both hydrogen atoms are transferred at the same time. It has also been proposed that a similar PT process can take place in the lowest triplet state, populated by non-radiative decay from the first excited singlet state.[26,29] As a consequence of these peculiar spectroscopic characteristics, this molecule has been recommended as a fluorescence standard,[24] a laser dye[25] and as a solar energy collecting material.[27]

Some theoretical studies have been carried out using *ab initio* and semiempirical methods,[28,31–33] but these works are focused on the relative stabilities of di-enol and di-keto tautomers in the S_0 and S_1 states, and on the polarizabilities of $BP(OH)_2$ in the ground electronic state. No attempt has been made until now to extend these studies to investigate potential energy surfaces (PES) for excited electronic states, and there is no theoretical support for the proposed concerted ESPT mechanism.[24]

Elementary chemical intuition suggests two possible mechanisms for tautomerization, depending on the concerted or successive transfer of the two protons. Transfer of a single proton would lead to a neutral structure with a non-zero dipole moment, whereas double PT produces a zwitterionic structure with a vanishing dipole moment (see Scheme 1). These structures are very well known in hydroxy-N-heteroaromatic compounds[34] and are stabilized in polar media. Moreover a torsional motion of the molecule taking place along the PT reaction path, *e.g.* a twisting between the two aromatic rings or a ring distortion, can play a significant role, especially in non-radiative decay.[24]

In an attempt to gain further insight into the above points, we have investigated, using semiempirical techniques, the possibility of tautomerization ruled by intramolecular PT in $BP(OH)_2$, both in the ground and excited electronic states, and its relationship with the UV spectra.

Computational details

The PT process has been investigated for the ground and first excited electronic states by AM1[35] and PM3[36] semiempirical methods, using the MOPAC 6.0[37] and HyperChem[38] packages. Ground state geometries have been fully optimized at the Hartree–Fock (HF) level. On the basis of previous experience,[18] the molecular geometries of stationary points on the lowest excited singlet (S_1) PES were optimized using a minimal configuration interaction (CI), including the ground state and the configurations obtained by exciting one or two electrons from the highest occupied molecular orbital (HOMO) to the lowest unoccupied molecular orbital (LUMO).[39] Using these geometries, more accurate energies were computed taking into account the 100 lowest energy configurations, obtained by exciting one or two electrons from the highest three occupied to the lowest two empty molecular orbitals. The so-called half-

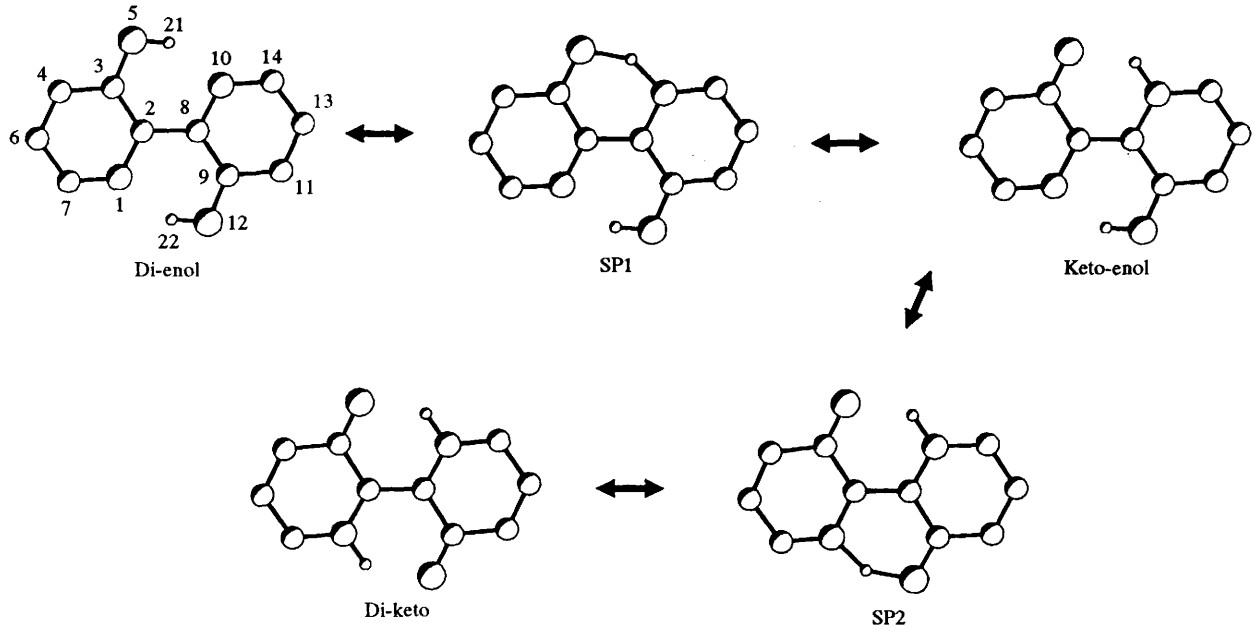

Fig. 1 Stationary points characterizing stepwise proton transfer in $BP(OH)_2$. The atom numbering is also shown.

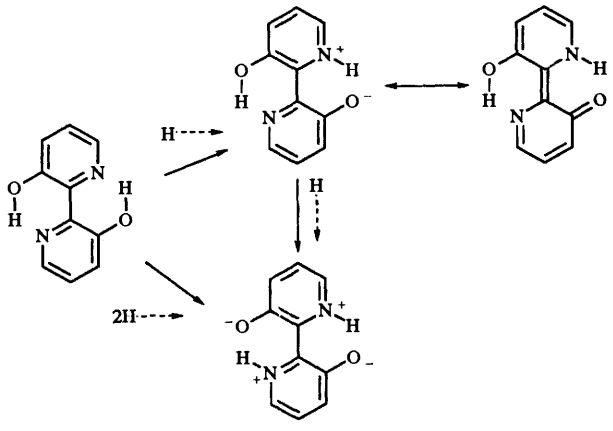

Scheme 1

electron approach[40] was used, instead, to determine geometric and energetic parameters of the lowest triplet state (T_1). All the energy minima and first order saddle points (SP) were characterized by computing harmonic frequencies. The PT mechanism in all the electronic states has been further characterized by tracing the so-called concerted reaction path (CRP),[41] which connects the reactant to the product through a linear modification of all Cartesian coordinates (*vide infra*). At energy minima some computations were carried out at the INDO/S level,[42] using the ARGUS package,[43] to evaluate S_0–S_1 transition energies.

Results and discussion

S_0 Electronic state

In Table 1 are reported the optimized geometric parameters for the di-enol [$BP(OH)_2$], and di-keto [$BP(NH)_2$] tautomeric forms, together with the available X-ray data. For the most stable di-enol species there is in general good agreement between PM3, *ab initio* and crystallographic data, especially as regards hydrogen bond parameters and the planarity of the molecule. In particular, PM3 computations predict a planar structure for the di-enol form, in agreement with experimental and previously published *ab initio* data.[33] On the contrary, AM1 calculations favour a twisted geometry, with a dihedral angle between the aromatic rings of *ca.* 60°. In this case, the planar structure is a first order saddle point, 7.5 kJ mol^{-1} higher in energy, with a transition vector corresponding to the torsion mode of one ring with respect to the other. Deviation from planarity affects, of course, the intramolecular hydrogen bond parameters. For instance the AM1 O–N distance (2.56 Å) is significantly shorter than the PM3 value (2.66 Å), whereas the OCC angle (127.6°) is larger than the PM3 (124.5°) and experimental (122°) values. On the other hand, the AM1 skeletal bond lengths and valence angles are very close to PM3 and experimental ones.

Also, in Table 1 are reported the geometric parameters for the di-keto form. Again, in this case the AM1 method predicts a twisted structure with a torsional angle of about 60°. This point is quite critical for the comprehension of the photochemical behaviour of $BP(OH)_2$. In fact, it has been suggested[24] that the torsional motion of the two rings is responsible for the non-radiative decay between the S_1 and S_0 states of the di-keto tautomer. So the availability of reliable structural information is a crucial point in the study of this molecule. Moreover, there are in the literature some indications that PM3 performs at least as well as the AM1 method in the evaluation of geometric and energetic parameters of tautomeric equilibria involving heterocyclic molecules.[44] On this basis, we have chosen to use systematically only the PM3 method for the study of the tautomeric reaction in all the considered electronic states.

The PM3 results correctly reproduce the expected zwitter-ionic structure (as reported in Scheme 1) of the di-keto tautomer. In fact, in going from the di-enol to the di-keto form there is a slight rearrangement involving all the ring bond distances, due to a new electronic distribution. There is also a sensible variation in the C–O bond length, which goes from 1.35 to 1.25 Å, in the di-enol and di-keto forms, respectively (*i.e.* from a single to a nearly double bond).

In Table 2 are reported some relevant geometric parameters of all the stationary points (minima and saddle points) characterizing the PM3 potential energy surface for the tautomerization reactions. Experimental data have been interpreted in terms of a concerted reaction mechanism (see Scheme 1). We localized a symmetric SP for the concerted mechanism, but computation of harmonic frequencies gives two imaginary frequencies, thus characterizing this stationary point as a second order saddle. Starting from this structure and

Table 1 Geometric parameters (Å and deg) of the two limiting tautomers of [2,2′-bipyridyl]-3,3′-diol in their ground electronic states

	Di-enol				Di-keto		
	AM1	PM3	*ab-initio*	Exp.	AM1	PM3	*ab-initio*
N(1)–C(2) N(10)–C(8)	1.36	1.37	1.33	1.34	1.36	1.37	1.34
C(2)–C(3) C(8)–C(9)	1.43	1.41	1.41	1.41	1.47	1.46	1.43
C(3)–C(4) C(9)–C(11)	1.42	1.41	1.39	1.38	1.45	1.45	1.42
C(4)–C(6) C(11)–C(13)	1.38	1.38	1.38	1.36	1.37	1.36	1.37
C(6)–C(7) C(13)–C(14)	1.41	1.40	1.38	1.37	1.41	1.41	1.39
C(7)–N(1) C(14)–N(10)	1.34	1.34	1.31	1.33	1.33	1.35	1.32
C(3)–O(5) C(9)–O(12)	1.36	1.35	1.33	1.34	1.26	1.25	1.25
O(5)–H(21) O(12)–H(22)	0.97	0.97	0.96	1.00	1.90	1.78	1.67
C(2)–C(8)	1.49	1.47	1.45	1.47	1.48	1.46	1.46
O(5)–N(10) O(12)–N(1)	2.56	2.66	2.65		2.69	2.60	2.56
N(1)–H(22) N(10)–H(21)	1.67	1.80	1.82		1.02	1.01	1.03
O(5)–C(3)–C(2) O(12)–C(9)–C(8)	127.6	124.5	124.7	122.0	123.3	121.6	121.9
C(3)–C(2)–C(8) C(9)–C(8)–C(2)	123.4	123.7	123.0	122.2	122.8	122.2	122.6
N(1)–C(2)–C(8) N(10)–C(8)–C(2)		116.5	116.8	117.1	117.9	118.2	116.9
H(21)–O(5)–C(3) H(22)–O(12)–C(9)	110.1	107.7	109.0	105.0		—	
H(21)–N(10)–C(8) H(22)–N(1)–C(2)			—			116.8	

Table 2 Geometric parameters (Å and deg) of all stationary points characterizing the tautomerization of [2,2′-bipyridyl]-3,3′-diol in the ground electronic state, according to PM3 computations

	Di-enol	SP1	Keto–Enol	SP2	Di-keto
N(1)–C(2)	1.37	1.37	1.39	1.38	1.37
N(10)–C(8)		1.37	1.38	1.36	
C(2)–C(3)	1.41	1.43	1.45	1.45	1.46
C(8)–C(9)		1.42	1.44	1.45	
C(3)–C(4)	1.41	1.43	1.46	1.45	1.45
C(9)–C(11)		1.40	1.39	1.42	
C(4)–C(6)	1.38	1.37	1.35	1.36	1.36
C(11)–C(13)		1.39	1.41	1.38	
C(6)–C(7)	1.40	1.41	1.43	1.42	1.41
C(13)–C(14)		1.39	1.37	1.39	
C(7)–N(1)	1.34	1.33	1.32	1.33	1.35
C(14)–N(10)					
C(3)–O(5)	1.35	1.30	1.25	1.25	1.25
C(9)–O(12)		1.35	1.35	1.30	
O(5)–H(21)	0.97	1.34	1.77	1.79	1.78
O(12)–H(22)		0.97	0.97	1.29	
C(2)–C(8)	1.47	1.46	1.43	1.45	1.46
O(5)–N(10)	2.66	2.48	2.59	2.61	2.60
O(12)–N(1)		2.67	2.63	2.46	
N(1)–H(22)	1.80	1.80	1.78	1.02	1.01
N(10)–H(21)		1.26	1.02	1.28	
O(5)–C(3)–C(2)	124.5	122.0	122.2	121.5	121.6
O(12)–C(9)–C(8)		123.3	123.1	120.9	
C(3)–C(2)–C(8)	123.7	121.0	122.7	122.8	122.2
C(9)–C(8)–C(2)		124.4	124.2	121.0	
N(1)–C(2)–C(8)	116.5	115.7	116.8	115.7	118.2
N(10)–C(8)–C(2)		117.4	118.2	118.8	
H(21)–O(5)–C(3)	107.7	106.4	—	—	—
H(22)–O(12)–C(9)		107.7	108.1	107.4	
H(21)–N(10)–C(8)	—	110.0	116.7	116.2	116.8
H(22)–N(1)–C(2)		—	—	109.0	

removing symmetry constraints, we localized and characterized as a true energy minimum the intermediate structure corresponding to the transfer of a single proton [hereafter keto–enol form, BP(OHNH)]. From this stable intermediate we also locate the two first order SPs corresponding to the stepwise PTs. All these structures are reported in Fig. 1. Some geometric parameters can be considered as indicative of the suggested stepwise mechanism. For instance the C(2)–C(8) distance decreases in going from the di-enol (1.46 Å) to the keto–enol (1.43 Å) form and successively increases in the di-keto form (1.46 Å). This situation corresponds to single–double–single bond exchange in the successive structures. There is also some correspondence between the O–N distance and the ongoing PT. In fact, one of the two O–N distances which is 2.66 Å in the di-enol form, decreases to 2.48 Å in the first SP and increases back to 2.59 Å in the intermediate, while the other O–N bond length is nearly constant during the first PT. The roles are exchanged in the second PT. A significant variation of the C(3)C(2)C(3) and C(9)C(8)C(2) angles accompanies PT.

The energetics of the suggested stepwise mechanism are summarized in Table 3. As mentioned above the PM3 results for the ground state are satisfactory, especially as regards the endothermicities of the tautomerization reaction. The HF computations indicate that the di-keto form is less stable by about 74 and 10 kJ mol^{-1} with respect to the di-enol and the keto–enol form, respectively. Inclusion of correlation energy makes the di-keto and keto–enol structures nearly isoenergetic. The activation energies for the two step mechanism are very high (114 and 150 kJ mol^{-1}), thus ruling out a PT mechanism passing through fully relaxed structures. On the other hand it is well known that this is not the most probable reaction path for

Table 3 Endothermicities (ΔE_1 and ΔE_2) and activation energies ($\Delta E^{\ddagger 1}$ and $\Delta E^{\ddagger 2}$) (kJ mol^{-1}) for the stepwise tautomerization of [2,2′-bipyridyl]-3,3′-diol in the S_0, S_1 and T_1 electronic states. The energy reference is always the di-enol form

	S_0			S_1		T_1	
	HF	CI	CI + ZPE	CI	CI + ZPE	CI	CI + ZPE
$\Delta E^{\ddagger 1}$	114.3	126.9	91.6	76.1	40.2	82.7	46.6
ΔE^1	64.6	73.2	71.1	−31.6	−39.6	−28.9	−35.6
$\Delta E^{\ddagger 2}$	149.7	154.7	118.3	63.2	24.7	62.1	20.6
ΔE^2	74.3	74.1	74.1	−20.0	−24.2	−35.4	−42.1

PT processes (*vide infra*). Zero point energies have a negligible effect on reaction energies, but strongly reduce activation barriers. Since this effect is (also quantitatively) very similar for all the electronic states, it will not be discussed again in the following sections. In any case, also taking into account ZPE effects, the energy barriers in the S_0 state remain sufficiently high to rule out significant intramolecular PT.

S_1 electronic state

A molecular orbital analysis shows that the S_0–S_1 transition is of the π–π^* type and is well represented by an HOMO–LUMO excitation. In Table 4 are collected the PM3 geometrical parameters for all the stationary points characterizing the S_1 surface. It is noteworthy that electronic excitation induces only small geometrical changes in the di-keto form, whereas some modifications [especially in the N(1)–C(2), C(2)–C(3) and C(2)–C(8)] bond lengths are found for the di-enol tautomer.

Table 4 Geometric parameters (Å and deg) of all stationary points characterizing the tautomerization of [2,2′-bipyridyl]-3,3′-diol in the S_1 electronic state, according to PM3 computations

	Di-enol	SP1	Keto–Enol	SP2	Di-keto
N(1)–C(2)	1.40	1.36	1.34	1.38	1.39
N(10)–C(8)		1.41	1.42	1.40	
C(2)–C(3)	1.44	1.46	1.47	1.46	1.46
C(8)–C(9)		1.41	1.38	1.44	
C(3)–C(4)	1.41	1.43	1.43	1.45	1.44
C(9)–C(11)		1.41	1.42	1.42	
C(4)–C(6)	1.39	1.38	1.38	1.37	1.37
C(11)–C(13)		1.40	1.41	1.39	
C(6)–C(7)	1.41	1.41	1.39	1.41	1.40
C(13)–C(14)		1.38	1.37	1.39	
C(7)–N(1)	1.34	1.36	1.37	1.35	1.36
C(14)–N(10)		1.36	1.39	1.37	
C(3)–O(5)	1.34	1.29	1.26	1.25	1.25
C(9)–O(12)		1.35	1.36	1.30	
O(5)–H(21)	0.98	1.23	1.75	1.84	1.79
O(12)–H(22)		0.96	0.96	1.31	
C(2)–C(8)	1.42	1.44	1.46	1.44	1.43
O(5)–N(10)	2.63	2.42	2.59	2.64	2.61
O(12)–N(1)		2.74	2.63	2.46	
N(1)–H(22)	1.77	1.90	1.79	1.27	1.01
N(10)–H(21)		1.30	0.99	1.01	
O(5)–C(3)–C(2)	123.7	121.3	120.2	121.3	121.4
O(12)–C(9)–C(8)		123.3	123.6	120.9	
C(3)–C(2)–C(8)	123.6	119.5	125.3	123.6	123.7
C(9)–C(8)–C(2)		125.8	126.8	121.7	
N(1)–C(2)–C(8)	116.9	119.4	113.5	115.2	117.7
N(10)–C(8)–C(2)		115.6	114.1	118.9	
H(21)–O(5)–C(3)	108.7	108.9	—	—	—
H(22)–O(12)–C(9)		108.2	106.2	106.9	
H(21)–N(10)–C(8)	—	108.5	116.0	116.3	116.9
H(22)–N(1)–C(2)		—	—	109.4	

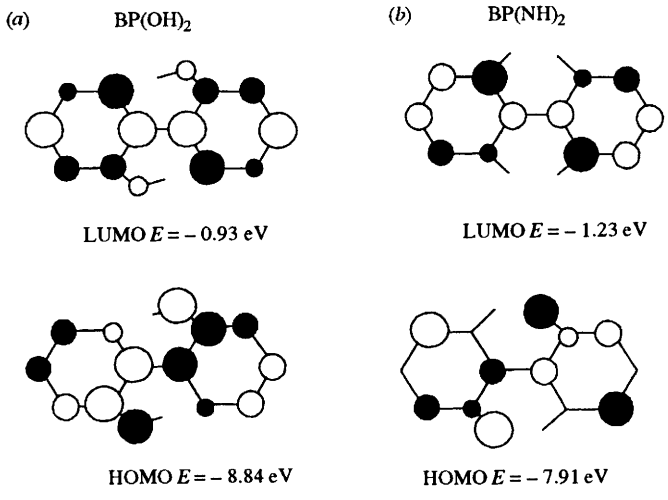

Fig. 2 Composition of frontier orbitals in (*a*) $BP(OH)_2$ and (*b*) $BP(NH)_2$ tautomers.

As in the case of the S_0 PES, it was possible to locate and characterize all the stationary points corresponding to the suggested stepwise PT mechanism. Also in these cases there are no significant geometrical variations with respect to ground state geometries. In the S_1 electronic state, the di-keto form is strongly stabilized and the whole PT process is exothermic by about 20 kJ mol^{-1}, while the intermediate keto–enol form does not change its relative energy. The electronic excitation also influences energy barriers, leading to an activation energy of about 76 kJ mol^{-1} for the first PT process and about 63 kJ mol^{-1} for the second.

The electronic origin of energetic and geometrical variations accompanying S_0–S_1 excitation is well evidenced on inspection of the frontier orbitals of the two tautomeric forms (see Fig. 2). The HOMOs of the two tautomers are very similar to one another. They correspond mainly to bonding contributions of the 2pπ atomic orbitals of N(1), C(2), C(3), C(4) and C(6) and C(7), together with the corresponding symmetric interactions, with an antibonding interaction with the 2pπ orbital of the oxygen atom. The HOMO energy of the di-enol form is lower by about 0.9 eV, due to a stronger N(1)–C(2)–C(3)–C(4) bonding interaction. On the contrary, LUMOs are dominated by antibonding interactions, with only small bonding contributions involving adjacent pairs of atoms. Since these contributions are more important in the di-keto form than in the di-enol one, the LUMO energy of the former tautomer is lower by about 0.2 eV. These effects are responsible for the stabilization of the di-keto form with respect to the di-enol form upon excitation from S_0 to S_1. It is also noteworthy that the LUMO orbitals of both tautomers are characterized by a strong π–π interaction between the C(2) and C(8) atoms, which enforces the planarity of the two tautomers in the S_1 state.

The shape of the frontier orbitals also shows a different character in the region of PT, *i.e.* on nitrogen and oxygen atoms. In fact, the contribution of nitrogen atoms is very small in the HOMO; in the LUMO, on the contrary, this position becomes electron-rich. The opposite behaviour is observed for oxygen atoms: electron density flows away from them when passing from the HOMO to the LUMO. From a chemical point of view, this means that in the first excited singlet state the nitrogen atom is a better Lewis base than in the ground electronic state, and that the hydroxylic oxygen is more acidic under excitation to the singlet state. These effects provide the driving force for the PT reaction in the S_1 electronic state.

T_1 electronic state

The optimized geometrical parameters of the tautomers in their T_1 electronic states are reported in Table 5. There are some significant variations of the geometries in going from the S_0 to the T_1 electronic state. For all tautomers the N(1)–C(2) and C(2)–C(3) bond lengths are longer than in the ground state, whereas the C(2)–C(8) distance is shorter. For instance in the di-enol form the first bond length is 0.06 Å longer in the T_1 than in the S_0 state, whereas the C(2)–C(8) distance increases from 1.38 (S_0) to 1.47 Å (T_1). These geometry differences (and other smaller ones) are due to the contribution of the LUMO, which has a repulsive anti-bonding character in the N(1)–C(2) and C(2)–C(3) regions and a bonding character in the C(2)–C(8) region.

In the T_1 electronic state the di-enol form is strongly destabilized, leading to a significant reduction of both endothermicities and activation energies. In particular, both keto–enol and di-enol forms are more stable than the di-keto tautomer (by 29 and 35 kJ mol^{-1}, respectively) whereas the activation energies are reduced to 83 and 62 kJ mol^{-1} for the first and second PT, respectively. These energy barriers are similar to those obtained for the S_1 state and significantly lower than those evaluated for the S_0 state, thus suggesting that some PT can take place in the excited electronic states.

Proton transfer mechanism

The choice of the reaction path governing the PT processes is not trivial. In the absence of strong curvature effects, the Intrinsic Reaction Path (IRP)[45,46] passing through first order saddle points provides an invaluable reference. In fact, each downhill segment of this path corresponds to an infinitely damped classical trajectory along which an infinite frictional force continuously damps the local energy to zero. On the other hand, heavy–light–heavy systems, like those considered in this study, are characterized by medium to strong curvatures.[47,48] In such circumstances, pending multidimensional studies, a

Table 5 Geometric parameters (Å and deg) of all stationary points characterizing the tautomerization of [2,2'-bipyridyl]-3,3'-diol in the T_1 electronic state, according to PM3 computations

	Di-enol	SP1	Keto–Enol	SP2	Di-keto
N(1)–C(2)	1.43	1.41	1.36	1.40	1.42
N(10)–C(8)		1.44	1.42	1.42	
C(2)–C(3)	1.47	1.48	1.49	1.49	1.49
C(8)–C(9)		1.45	1.43	1.46	
C(3)–C(4)	1.40	1.42	1.45	1.45	1.45
C(9)–C(11)		1.39	1.40	1.43	
C(4)–C(6)	1.38	1.38	1.37	1.37	1.37
C(11)–C(13)		1.40	1.41	1.39	
C(6)–C(7)	1.43	1.41	1.40	1.40	1.40
C(13)–C(14)		1.40	1.38	1.39	
C(7)–N(1)	1.32	1.33	1.36	1.36	1.37
C(14)–N(10)		1.34	1.38	1.37	
C(3)–O(5)	1.34	1.29	1.24	1.24	1.24
C(9)–O(12)		1.34	1.34	1.28	
O(5)–H(21)	0.97	1.27	1.84	1.86	1.82
O(12)–H(22)		0.97	0.97	1.27	
C(2)–C(8)	1.38	1.39	1.42	1.39	1.38
O(5)–N(10)	2.65	2.45	2.64	2.65	2.62
O(12)–N(1)		2.68	2.64	2.44	
N(1)–H(22)	1.79	1.82	1.79	1.19	1.01
N(10)–H(21)		1.29	1.01	1.01	
O(5)–C(3)–C(2)	123.0	120.6	121.7	120.5	120.6
O(12)–C(9)–C(8)		121.8	123.2	120.3	
C(3)–C(2)–C(8)	124.7	121.4	122.8	124.0	124.1
C(9)–C(8)–C(2)		125.8	123.2	121.6	
N(1)–C(2)–C(8)	117.8	118.9	122.8	116.0	118.1
N(10)–C(8)–C(2)		116.3	124.3	120.1	
H(21)–O(5)–C(3)	108.3	108.0	—	—	—
H(22)–O(12)–C(9)		108.2	108.8	108.5	
H(21)–N(10)–C(8)	—	107.5	116.7	115.7	116.4
H(22)–N(1)–C(2)		99.0	—	109.0	

better reference is often provided by the so-called Concerted Reaction Path (CRP), which is obtained assuming a linear variation of geometrical parameters between reactants and products.[41]

Another problem is the choice of the geometries of the minima from which to determine the path. Generally in spectroscopic studies geometries optimized for the ground electronic state have been used also for excited states (see for instance ref. 40), assuming a Franck–Condon-like excitation process. This procedure is, however, questionable, since upon excitation, but prior to PT, the system has the time to relax its geometry to that characterizing the electronic state of interest.[21]

As a first step we built the CRP for the double PT reaction in the S_0 and S_1 electronic states, using the ground state geometries. We obtained energy barriers of 224 and 161 kJ mol^{-1}, for the S_0 and S_1 state, respectively. These barriers are very high and rule out a tautomerization process driven by a PT mechanism, in both electronic states. So we devoted our attention to the stepwise mechanism. In Figs. 3, 4 and 5 are reported the CRPs obtained for the first three electronic states using S_0, T_1 and S_1 geometries, respectively. For each path we have explicitly computed ten points between the di-keto and keto–enol energy minima and another ten points from there to the di-enol minimum. Continuous curves have been then obtained through spline interpolations. Note that the distance along the CRP depends on the values assigned to the three energy minima (here 0.0, 0.5 and 1.0 arbitrary units). It is quite apparent that all the electronic states are characterized by a well defined intermediate, corresponding to the keto–enol form. Moreover the structures of all the stationary points (minima and SPs) are quite similar to those obtained by complete geometry optimizations.

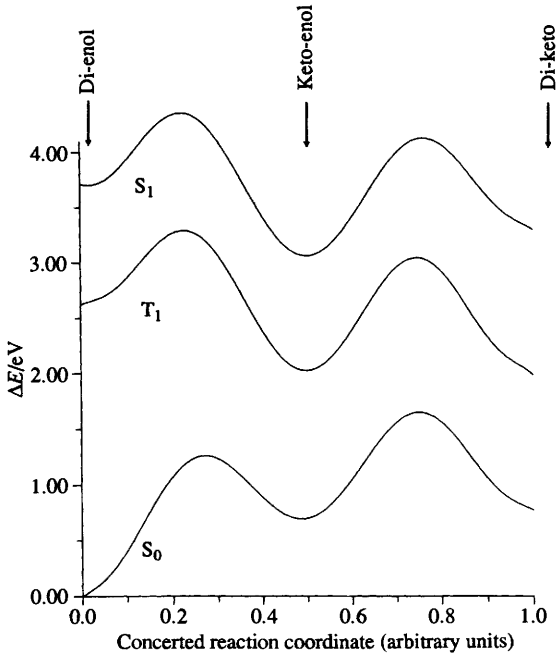

Fig. 3 Concerted reaction paths for the stepwise proton transfer reaction in $BP(OH)_2$. The paths refer to S_0, S_1 and T_1 electronic states and are computed using the geometries of energy minima optimized for the S_0 state.

The CRPs of all the electronic states are not significantly altered when determined from S_1, T_1 or S_0 geometries of reactants and products. In fact, the S_0 state is always characterized by quite high energy barriers (126, 91 and 117 kJ mol^{-1} for the profiles computed using the S_0, T_1 and S_1 geometries) and reaction energies (64, 31 and 92 kJ mol^{-1} for the same profiles) for the first PT. The activation energies decrease for the second PT (20, 97 and 66 kJ mol^{-1}), and the second step is slightly endothermic (7 and 30 kJ mol^{-1} with the S_0 and the T_1 geometries, respectively) or exothermic (24 kJ mol^{-1} for the S_1 geometry profiles).

The energy barriers to the first PT decrease in the T_1 electronic state and the first activation energies are smaller or equal to the second ones. Moreover, the keto–enol form is significantly stabilized with respect to the di–enol tautomer, and the whole tautomerization is slightly exothermic. In fact the activation energies for the first PT range between 60 (using the S_0 geometry) and 93 kJ mol^{-1} (with the T_1 geometry), while the corresponding second activation energies are 98 and 105 kJ mol^{-1}. On the other hand, both keto–enol and di–keto forms are strongly stabilized in all cases, the first PT being exothermic by 65, 29 and 39 kJ mol^{-1}, and the second PT exothermic by 3, 7 and 6 kJ mol^{-1} for the S_0, T_1 and S_1 profiles, respectively. The second activation energies are nearly identical for all the profiles. A similar behaviour is observed in the S_1 electronic state, where the first and second activation energies are roughly equal and the keto–enol form is always stabilized.

The overall tautomerization mechanism can be summarized as follows. PT is quite unlikely in the S_0 state, the first activation energy being very high. If the molecule is excited in the S_1 or T_1 states through a vertical process, the activation energy strongly decreases and the keto–enol form is stabilized. So the first PT is favoured from both kinetic and thermodynamic points of view. On the other hand, the presence of a significant energy barrier for the second PT seems to indicate that the rate determining step is the second proton transfer (see Fig. 3), which is (however) slightly exothermic.

Upon geometry relaxation in the S_1 state, there is a significant increase of the energy barrier for the S_1 and T_1 states, and a

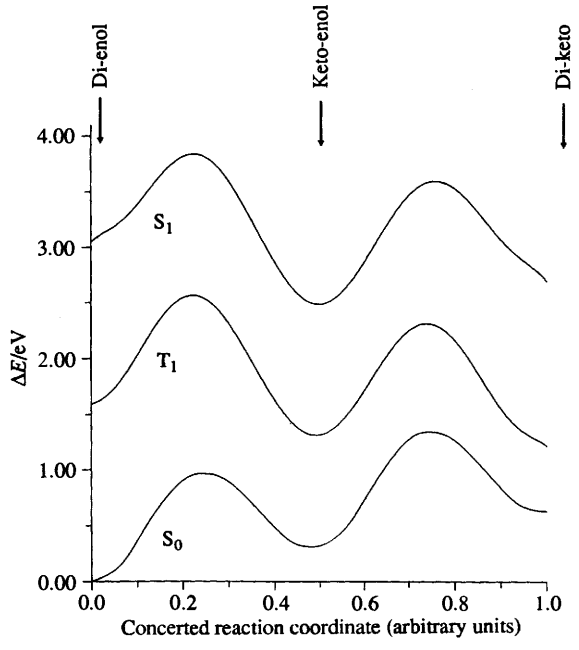

Fig. 4 Concerted reaction paths for the stepwise proton transfer reaction in $BP(OH)_2$. The paths refer to S_0, S_1 and T_1 electronic states and are computed using the geometries of energy minima optimized for the T_1 state.

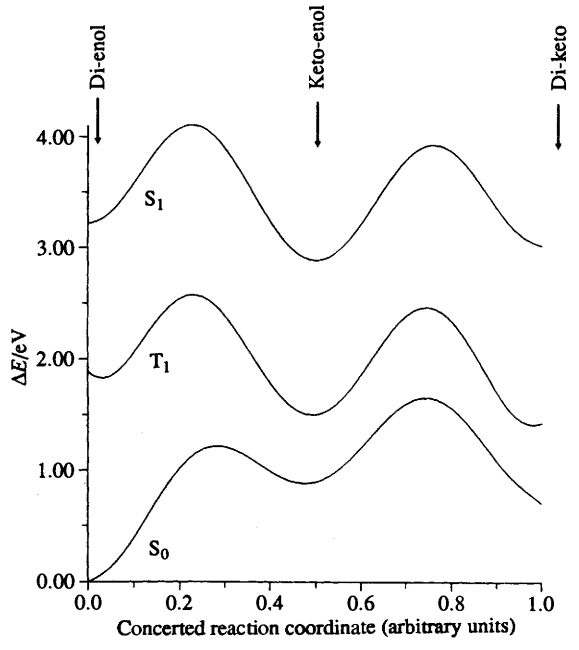

Fig. 5 Concerted reaction paths for the stepwise proton transfer reaction in $BP(OH)_2$. The paths refer to S_0, S_1 and T_1 electronic states and are computed using the geometries of energy minima optimized for the S_1 state.

slight stabilization of the keto–enol form. This suggests that the process is less probable after geometrical relaxation, even if, especially in the T_1 state, possible (see Fig. 4). On the other hand, in the S_0 state the reverse di-keto–di-enol interconversion is favoured, since the first activation energy is quite low and the keto–enol form is strongly destabilized. High energy barriers and small stabilization of the keto–enol form seem to exclude a PT mechanism in the relaxed T_1 state, and also after vertical decay to S_0.

In summary, it can be suggested that the di-enol–di-keto interconversion in $BP(OH)_2$ is ruled by a stepwise PT, characterized by a well defined intermediate keto–enol form.

Table 6 INDO/S spectral maxima (nm) and oscillator strengths for absorption and emission spectra of the [2,2′-bipyridyl]-3,3′-diol system in the gas-phase are compared with the available experimental data

	Abs.	Exp.[a]	Em.	Exp.[a]
Di-enol	335 (0.52)	345 (strong)	365 (0.56)	
Keto–Enol	495 (0.91)		557 (0.42)	
Di-keto	543 (0.60)		567 (0.62)	526 (strong)

[a] Ref. 26.

Since the first activation energies and the corresponding endothermicities are very high, the reaction is unlikely in the ground state, but a strong decrease of energy barriers upon vertical excitation to T_1 and S_1, makes the whole mechanism plausible for excited electronic states.

UV spectra

The INDO/S transition energies computed for the absorption and emission spectra of the different tautomers are reported in Table 6. Energy values refer to vertical transitions, starting from the PM3 optimized geometries of the ground state. Transition energies are in fairly good agreement with experiment. As mentioned in the introduction, the UV absorption spectrum of $BP(OH)_2$ shows a strong band centred around 345 nm, while the di-keto tautomer has one emission band centred at 526 nm. Both bands are well reproduced at the INDO/S level. In fact, the di-enol form shows an absorption centred at 335 nm, while the emission wavelength is red-shifted to 365 nm. On the other hand, the di-enol form has an emission at 567 nm, which corresponds to an absorption band centred at 543 nm. It must be noted that the di-keto and keto–enol forms have similar emission spectra (band maxima at 567 and 557 nm, respectively). This finding suggests that it is not possible to define experimental emission spectra as characteristic of the di-keto form.

Conclusions

In this paper we have reported the results of a comprehensive analysis of both concerted and stepwise PT in several electronic states of [2,2′-bipyridyl]-3,3′-diol.

From an experimental point of view this compound exists, in the ground electronic state, in the di-enol form and there is no evidence which would favour a double minimum potential for PT. Our calculations show, instead, that three energy minima should exist on the S_0 PES, corresponding to di-enol, keto–enol and di-keto forms. Contrary to chemical intuition, tautomerization is thus driven by a stepwise rather than concerted proton transfer. The energetics of the reaction are, however, compatible with the experimental findings. In fact the endothermicities of both PT steps are sufficiently high to prevent experimental observation of all forms but the di-enol one.

In the lowest excited electronic states the relative stabilities of di-enol and di-keto forms are reversed due to significant modifications of the acid–base properties of the oxygen and nitrogen atoms. As a consequence ESPT can occur. An important issue is, therefore, whether excited state tautomerization occurs with or without a barrier. From an experimental point of view one cannot observe, even at low temperatures, the fluorescence corresponding to primarily excited species, which indicates that initially excited structures decay too fast to emit a photon. Our computations show that PT is governed by significant activation barriers also in excited electronic states. Excess energies accumulated upon electron excitation (at least equal to energy differences between vertical and adiabatic excitations, *i.e.* 35 and 45 kJ mol^{-1} for S_1 and T_1, respectively)

are however very close or even higher than energy barriers including zero point energies (40.2 and 25.9 kJ mol^{-1} for the S_1 and T_1 states, respectively). As a consequence a fast PT occurs and fluorescence emission is observed only from the keto–enol or di-keto forms. Discrimination between these two species is difficult since the computed spectral patterns are very similar. In any event, the measurement of a zero dipole moment for the fluorescing species in the S_1 state [28] suggests a prevalence of the di-keto tautomer, and our PM3 computations suggest the same trend in the T_1 state.

From a more general point of view the present study suggests that structural interpretation of spectroscopic data requires great care, since different mechanisms (*e.g.* concerted PT or stepwise PT with a relatively unstable intermediate and a rate determined by the first step) can lead to the same experimental pattern. The level of the computations reported in the present paper is, of course, not sufficient to unambiguously solve a difficult mechanistic problem. It shows, however, that the presence of double minima and energy barriers govening PT in the different electronic states are not incompatible with the available experimental data. This points out once again the complementarity of experimental and theoretical (even semiempirical) approaches in the elucidation of complex physico-chemical processes.

References

1 P. F. Barbara, P. K. Walsh and L. E. Brus, *J. Phys. Chem.*, 1989, **93**, 29.
2 J. S. Kwiatkowski, T. J. Zielinski and R. Rein, *Adv. Quantum Chem.*, 1986, **18**, 85.
3 M. D. Topal and J. R. Fresco, *Nature*, 1976, **263**, 285.
4 W. G. Cooper, *Int. J. Quantum Chem.*, 1978, **14**, 71.
5 J. Rieker, E. Lemmert-Schmitt, G. Goeller, M. Roessler, G. J. Stueber, H. Schettler, H. E. A. Kramer, J. J. Stezowski, H. Hoier, S. Henkel, A. Schmidt, H. Port, M. Wiechmann, J. Rooly, G. Rytz, M. Slongo and J. L. Birbaum, *J. Phys. Chem.*, 1992, **96**, 10225.
6 D. A. Parthenopoulos, D. McMorrow and M. Kasha, *J. Phys. Chem.*, 1991, **95**, 2668.
7 P. Chou, D. McMorrow, T. J. Aartsma and M. Kasha, *J. Phys. Chem.*, 1984, **88**, 4596.
8 M. H. Van Benten and G. D. Gillispie, *J. Phys. Chem.*, 1984, **88**, 2954.
9 T. Nishiya, S. Yamauchi, N. Hirota, M. Baba and I. Hanazaki, *J. Phys. Chem.*, 1986, **90**, 5730.
10 J. Goodman and L. E. Brus, *J. Am. Chem. Soc.*, 1978, **100**, 7472.
11 P. F. Barbara, P. K. Walsh and L. E. Brus, *J. Phys. Chem.*, 1989, **93**, 29.
12 A. Peluso, C. Adamo and G. Del Re, *J. Math. Chem.*, 1992, **10**, 249.
13 A. Mordzinski and W. Kuhle, *J. Phys. Chem.*, 1986, **90**, 1455.
14 A. Muhlpfordt, T. Bultmann, N. P. Ernsting and B. Dick, *Chem. Phys.*, 1994, **181**, 447.
15 H. B. Schlegel, P. Gund and E. M. Fluder, *J. Am. Chem. Soc.*, 1982, **104**, 5347.
16 M. J. Field and I. H. Hillier, *J. Chem. Soc., Perkin Trans. 2*, 1987, 617.
17 L. Adamowicz, *Chem. Phys. Lett.*, 1989, **161**, 73.
18 C. Adamo, V. Barone, S. Loison and C. Minichino, *J. Chem. Soc., Perkin Trans. 2*, 1993, 697.
19 V. Barone and C. Adamo, *J. Comput. Chem.*, 1994, **15**, 385.
20 V. Barone and C. Adamo, *J. Photochem. Photobiol. A*, 1994, **80**, 211.
21 V. Barone and C. Adamo, *Chem. Phys. Lett.*, 1994, **226**, 399.
22 D. D. Pant, H. C. Joshi, P. B. Bisht and H. B. Tripathi, *Chem. Phys. Lett.*, 1994, **185**, 137.
23 F. R. Prieto, M. C. R. Rodrigues, M. M. Gonzalez and M. A. R. Fernandez, *J. Phys. Chem.*, 1994, **98**, 8666.
24 H. Bulska, *Chem. Phys. Lett.*, 1983, **98**, 398.
25 J. Sepiol, H. Bulska and A. Grabowska, *Chem. Phys. Lett.*, 1986, **140**, 607.
26 J. Sepiol, A. Grabowska, H. Bulska, A. Mordzinski, F. Perez Salgado and R. P. H. Rettschnick, *Chem. Phys. Lett.*, 1989, **163**, 443.
27 M. Eyal, R. Reisfeld, V. Chernyak, L. Kaczmarek and A. Grabowska, *Chem. Phys. Lett.*, 1991, **176**, 531.
28 R. Wortmann, K. Elich, S. Lebus, W. Liptay, P. Borowicz and A. Grabowska, *J. Phys. Chem.*, 1992, **96**, 9724.
29 A. Grabowska, P. Borowicz, D. O. Martire and S. E. Braslavsky, *Chem. Phys. Lett.*, 1991, **185**, 206.
30 L. Kaczmarek, B. Nowak, J. Zukowski, P. Borowicz, J. Sepiol and A. Grabowska, *J. Mol. Struct.*, 1991, **248**, 189.
31 L. Kaczmarek, R. Balicki, J. Lipkowski, P. Borowicz and A. Grabowska, *J. Chem. Soc., Perkin Trans. 2*, 1994, 1603.
32 J. Waluk, H. Bulska, A. Grabowska and A. Mordzinski, *New J. Chem.*, 1986, **10**, 413.
33 J. Lipkowski, A. Grabowska, J. Waluk, G. Calestani and B. A. Hess, *J. Crystallogr. Spectrosc. Res.*, 1992, **22**, 563.
34 S. F. Mason, J. Philip and B. E. Smith, *J. Chem. Soc. A*, 1968, 3051.
35 M. J. S. Dewar, E. G. Zoebisch, E. F. Healy and J. J. P. Stewart, *J. Am. Chem. Soc.*, 1985, **107**, 3902.
36 J. J. P. Stewart, *J. Comput. Chem.*, 1989, **10**, 221.
37 J. J. P. Stewart, MOPAC 6.0, Quantum Chemistry Program Exchange, Program no. 452.
38 HyperChem v. 3.0, HyperCube Inc.
39 M. J. S. Dewar, M. A. Fox, K. A. Campbell, C. C. Chen, J. B. Friedheim, M. K. Halloway, S. C. Kim, P. B. Lieschesky, A. M. Pakiari, T. P. Tien and E. G. Zoebisch, *J. Comput. Chem.*, 1984, **5**, 480.
40 M. J. S. Dewar, J. A. Hashmall and C. G. Venier, *J. Am. Chem. Soc.*, 1968, **90**, 1953.
41 A. L. Sobolewski, *Chem. Phys. Lett.*, 1993, **211**, 293.
42 J. Ridley and M. A. Zerner, *Theor. Chim. Acta*, 1973, **32**, 111.
43 M. A. Thompson, ARGUS v. 1.1; M. A. Thompson and M. C. Zerner, *J. Am. Chem. Soc.*, 1990, **112**, 7828.
44 W. M. F. Fabian, *J. Comput. Chem.*, 1991, **12**, 17.
45 K. Fukui, *J. Phys. Chem.*, 1970, **74**, 4161.
46 K. Fukui, *Acc. Chem. Res.*, 1981, **14**, 363.
47 W. H. Miller, N. C. Handy and J. E. Adams, *J. Chem. Phys.*, 1980, **72**, 99.
48 B. C. Garrett, D. G. Truhlar, R. S. Grew and A. W. Magnusson, *J. Phys. Chem.*, 1980, **84**, 1730.

Paper 4/06733I
Received 3rd *November* 1994
Accepted 3rd *February* 1995